physiologically based model for modeling an inverse system [12]. However, only the partial aspects of the nonlinearities were compensated and consequently the output system still had some oscillatory responses if the extent of a certain posture of FES motions such as standing or walking exceeds the range of the compensated linearity. Thus, we try to completely compensate the nonlinearities of a knee joint musculoskeletal model through feedback linearization with inverse compensation scheme and to suggest a new linear control scheme for tracking the reference trajectory of FES posture related with knee joint movements.

2. KNEE JOINT MUSCULOSKELETAL MODEL

The musculoskeletal system model of a knee joint with quadriceps muscle, which has an important role in FES standing, walking and cycling, is depicted as three blocks as shown in Fig. 1.

In Fig. 1, the first block contains the recruitment feature of muscle fibers, $r(s)$ stimulated by the intensity s, which is formulated in (1).

$$r(s) = s_c \tanh(s_h(s - x_c)) + y_c . \quad (1)$$

Here, the parameters of a rising and a falling path are not identical and they represent the different hysteretic characteristics depending on the path, i.e.,

i) On a rising path: $s_c = s_{rc}, s_h = s_{rh}, x_c = x_{rc}, y_c = y_{rc}$,

ii) On a falling path: $s_c = s_{fc}, s_h = s_{fh}, x_c = x_{fc}, y_c = y_{fc}$.

The first block also includes the 1st order activation dynamics of the muscle's normalized active state corresponding to the calcium release. The activation dynamics, $a(t)$ is described by

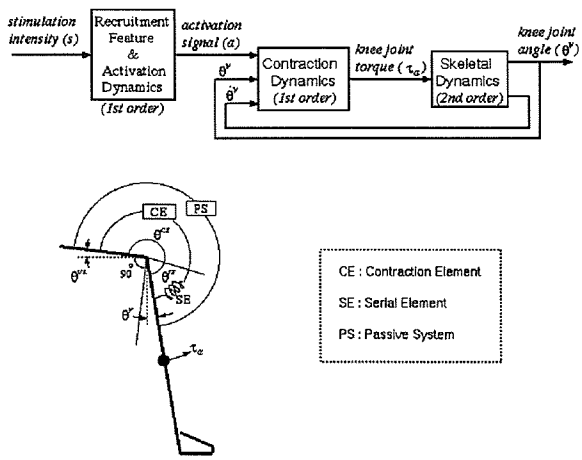

Fig. 1. A musculoskeletal system model of a knee joint.

$$\dot{a} = (r - a)r/\tau_r + (r - (a - a_{\min}) - (r - a)r)/\tau_f . \quad (2)$$

Here, the time constants of τ_r and τ_f are the different rates of calcium release to and uptake from muscle fibers, respectively and $a_{\min}$ is the minimal active state.

The second block in Fig. 1 includes the 1st order muscle contraction dynamics. We adopted a lumped model of musculotendon and a moment arm as indicated in the lower schematics of Fig. 1 to refer the muscle to a torque generator [13]. The contraction dynamics of the musculotendon was stated as

$$\dot{\tau}_a = (k_2\tau_a + k_1 k_2 \tau_{\max}) \cdot \left(-\dot{\theta}^V - \dot{\theta}^{CE}_{\max} g^{-1}_{CE}\left(\tau_a / \left(\tau_{\max} k_{CE}(\theta^{CE}) a\right)\right)\right), \quad (3)$$

where

$$\theta^{CE} = 3\pi/2 - (\theta^V + \theta^{UL}) - \ln\left(\tau_a/(\tau_{\max}k_1) + 1\right)/k_2,$$

$$k_1 = 1/\left(\exp(sh^{SE}) - 1\right), \quad k_2 = sh^{SE}/\theta^{SE}_{\max},$$

$$g^{-1}_{CE}(X) = \begin{cases} \dfrac{sh^{CEg}_{low}(X-1)}{X + sh^{CEg}_{low}} & (0 \le X < 1) \\ \dfrac{x_s sh^{CEg}_{up}(X-1)}{-X + y_s sh^{CEg}_{up} + y_s + 1} & (1 \le X < 1.3), \end{cases}$$

$$k_{CE}(Y) = \begin{cases} \exp\left(-\left(\dfrac{Y - \theta^{CE_L}_{\max}}{sh^{CEk_L}}\right)^2\right) & (Y < \theta^{CE}_{\max}) \\ (1 - c_1)\exp\left(-\left(\dfrac{Y - \theta^{CE_R}_{\max}}{sh^{CEk_R}}\right)^2\right) & \\ \quad + sl^{CEk}(Y - \theta^{CE_R}_{\max}) + c_1 & (\theta^{CE}_{\max} \le Y). \end{cases}$$

Here, τ_a is the active muscle torque, k_1 and k_2 are the parameters of series elastic element (SE). $\dot{\theta}^{CE}_{\max}$ is the maximum contraction velocity of the contractile element (CE), $g^{-1}_{CE}()$ is the inverse function of torque-angular velocity relationship of the CE, $\tau_{\max}$ is the maximum muscle torque and $k_{CE}()$ is the torque-angle relationship of the CE.

The third block of Fig. 1 can be described by the following 2nd order skeletal dynamics:

$$\ddot{\theta}^V = 1/I\left(\tau_a - G\sin(\theta^v) - D\dot{\theta}^V + s_1(e^{-s_2(\theta^V + \theta^{UL})} - 1)\right). \quad (4)$$

Here, θ^v is the knee joint angle with reference to the vertical line, I and G are the moment of inertia and the gravity constant of the lower leg, respectively. The latter term of (4), $-D\dot{\theta}^V + s_1(e^{-s_2(\theta^V + \theta^{UL})} - 1)$ represents the damping and elastic torque induced by the

Table 1. Knee joint, vastus lateralis muscle parameters used in our computer simulation.

s_{rc}	1.661	τ_r	0.02	$sh_{low}^{CE_g}$	0.25	sh^{CEk_R}	0.2
s_{rh}	2.346	τ_f	0.2	$sh_{up}^{CE_g}$	0.25	sl^{CEk}	-0.18
x_{rc}	1.143	$a_{\min}$	0.001	x_s	0.2	$\theta_{\max}^{CE}$	3.491
y_{rc}	1.538	sh^{SE}	2.7	y_s	0.3	I	0.44
s_{fc}	0.516	$\theta_{\max}^{SE}$	0.384	$\theta_{\max}^{CE_L}$	3.491	G	16.5
s_{fh}	7.054	θ^{UL}	0.154	sh^{CEk_L}	0.2	D	0.22
x_{fc}	0.792	$\tau_{\max}$	11.32	c_1	0.75	s_1	0.092
y_{fc}	0.536	$\dot{\theta}_{\max}^{CE}$	18	$\theta_{\max}^{CE_R}$	3.456	s_2	5.09

passive system, such that D, s_1, s_2 are the constants and θ^{UL} is the angle of the upper leg with reference to the horizontal line. The muscle contraction and skeletal dynamics stated in (3) and (4) can be alternatively expressed by the state space representation form as stated in (5) if we define $x_1 \equiv \tau_a$, $x_2 \equiv \theta^V$, $x_3 \equiv \dot{\theta}^V$ and the output variable, $y \equiv \theta^V$.

$$\begin{aligned}
\dot{x}_1 &= (k_2 x_1 + k_1 k_2 \tau_{\max}) \cdot \\
&\quad \left(-x_3 - \dot{\theta}_{\max}^{CE} g_{CE}^{-1}\left(x_1/\left(\tau_{\max} k_{CE}(x_1, x_2) a\right)\right)\right), \\
\dot{x}_2 &= x_3, \\
\dot{x}_3 &= 1/I\left(x_1 - G\sin(x_2) - Dx_3 + s_1\left(e^{-s_2(x_2+\theta^{UL})} - 1\right)\right), \\
y &= x_2. \qquad (5)
\end{aligned}$$

Thus the overall plant (musculoskeletal system) dynamics can be interpreted as a 4th order system composing of i) one activation dynamic unit, ii) one contraction dynamics unit, iii) two skeletal dynamics units. For our computer simulations, we adopted the estimated knee joint and vastus lateralis muscle parameters that are identified by the lump parameters for knee extensors for the voluntary contraction and for knee joints with the vastus lateralis muscle, respectively as stated in Table 1.

The identification procedures determining muscle parameters shown in Table 1 are listed in [13,16] and the accuracy of the model parameters are evaluated by tracking the model-predicted joint angle trajectories compared with experimental data [13].

3. NONLINEAR CONTROLLER DESIGN

The main control task of our study is to force a certain knee joint angle to track the reference trajectory. The overall control system structure is shown in Fig. 2.

The central idea of our suggested controller is utilizing a feedback linearization. In other words, we approximate a nonlinear system dynamics into a linear one with applying the algebraic transformation. With this scheme, the inherent nonlinearities contained in a musculoskeletal system model of the knee joint are vanished, and consequently the relatively simple linear control scheme can be applied. In Fig. 2, two inverse compensation units for the feedback linearization are described [17]. The first inverse compensation unit as stated in the following equation is to eliminate the nonlinearity of a term, $g_{CE}^{-1}\left(x_1/\left(\tau_{\max} k_{CE}(x_1, x_2) a\right)\right)$, which represents the muscle contraction dynamics.

$$r_{in} = \begin{cases} \dfrac{-x_1 u_{in} + sh_{low}^{CE_g} \dot{\theta}_{\max}^{CE} x_1}{sh_{low}^{CE_g} \tau_{\max} k_{CE}(x_1, x_2) u_{in} + sh_{low}^{CE_g} \dot{\theta}_{\max}^{CE} \tau_{\max} k_{CE}(x_1, x_2)} \\ \qquad \left(0 \le \dfrac{x_1}{\tau_{\max} k_{CE}(x_1, x_2) a} < 1\right) \\ \dfrac{x_1 u_{in} + x_s sh_{up}^{CE_g} \dot{\theta}_{\max}^{CE} x_1}{((y_s sh_{up}^{CE_g} + y_s + 1)\tau_{\max} u_{in} + x_s sh_{up}^{CE_g} \dot{\theta}_{\max}^{CE} \tau_{\max}) k_{CE}(x_1, x_2)} \\ \qquad \left(1 \le \dfrac{x_1}{\tau_{\max} k_{CE}(x_1, x_2) a} < 1.3\right) \end{cases} \qquad (6)$$

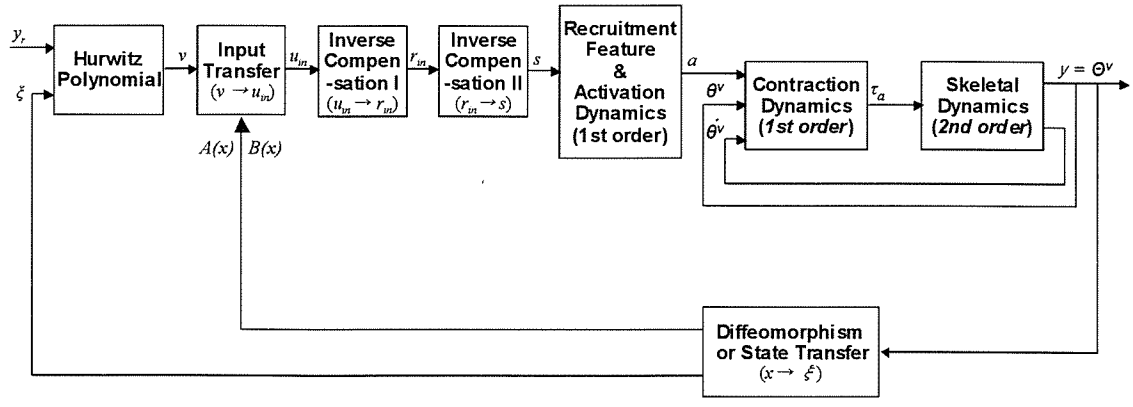

Fig. 2. The proposed control system structure.

In (6), u_{in} is the control input and required recruitment r_{in} is the output. The second inverse compensation unit as stated in the following equation is to remove the nonlinearity of the recruitment.

$$s = \ln\left(\left(r_{in} + (s_c - y_c)\right)/\left(-r_{in} + (s_c + y_c)\right)\right)/2s_h + x_c. \quad (7)$$

In (7), r_{in} is the input and the normalized stimulation intensity, s is the output. Since the normalized active state a in (2) is not measurable, it is regarded as a bounded and structured uncertainty. Then, the diffeomorphism (state transfer) [18] is defined as in (8) and the control law (input transfer) u_{in} is defined as in (9), respectively.

$$\begin{aligned} \xi_1 &\equiv y = x_2, \\ \xi_2 &\equiv \dot{y} = x_3, \\ \xi_3 &\equiv \ddot{y} = x_1/I - G\sin(x_2)/I - Dx_3/I \\ &\quad + s_1(\exp(-s_2(x_2 + \theta^{UL})) - 1)/I, \end{aligned} \quad (8)$$

$$u_{in} = (v - B(x))/A(x), \quad (9)$$

where

$$\begin{aligned} A(x) &\equiv -(k_2x_1 + k_1k_2\tau_{\max})/I, \\ B(x) &\equiv (k_2x_1 + k_1k_2\tau_{\max})(-x_3 + 1)/I - G\cos(x_2)x_3/I \\ &\quad - D(x_1/I - G\sin(x_2)/I - Dx_3/I \\ &\quad + s_1\left(\exp(-s_2(x_2 + \theta^{UL})) - 1\right)/I)/I \\ &\quad + s_1(-s_2\exp(-s_2(x_2 + \theta^{UL}))x_3)/I. \end{aligned}$$

(9) is derived by combining the diffeomorphism of (8) and the control law. The input to the control law v is selected as stated in (10) and (11),

$$\dddot{y} = v, \quad (10)$$

$$v = \ddot{y}_r + \alpha_2(\ddot{y}_r - \xi_3) + \alpha_1(\dot{y}_r - \xi_2) + \alpha_0(y_r - \xi_1), \quad (11)$$

where $\alpha_2, \alpha_1, \alpha_0$ are the coefficients of the Hurwitz polynomial $s^3 + \alpha_2 s^2 + \alpha_1 s + \alpha_0$. The Hurwitz polynomial coefficients are chosen with considering the behavior and response of the closed-loop system in terms of overshoot, rising time and settling time. Since the degree of the control system is three, we need to differentiate the output three times to get the control input.

The reference trajectory $y_r(t)$ was set as a sinusoidal function, which is useful in clinical practice because it is often used for paralyzed muscle training. The simulation result is shown in Fig. 3. With the inverse compensations of nonlinearities and the feedback linearization stated above, the stable output tracking of the overall closed-loop system was successfully achieved.

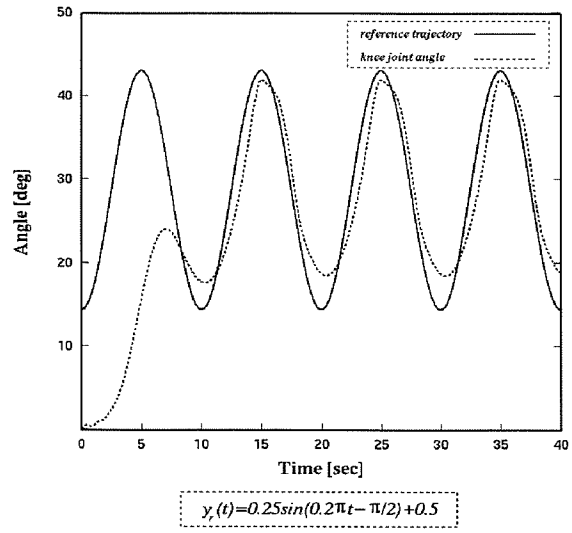

Fig. 3. The simulation result of FES nonlinear control.

4. CONCLUSIONS

As we mentioned earlier, the recent closed-loop control schemes for FES do not completely compensate the nonlinearities of the plant and consequently often lead to the oscillatory responses. Our control plant shows better performance in terms of output tracking. Also, the output of the control system achieves the stable conditions by utilizing a feedback linearization with considering inverse compensations. Thus, we believe that we have suggested a new promising application especially for controlling the inherent nonlinearity of the FES system. In other words, we propose a new nonlinear control scheme to track a referenced angle trajectory of the paralyzed knee joint with implementing a controller composing two linearization units.

For the real clinical application of our control scheme, the following two issues must be considered. Firstly, the model parameters must be easily identified so that we can minimize the physical and psychological burdens of a patient. Secondly, the control scheme must be improved to be adaptive to time varying factors in the musculoskeletal system such as muscle fatigue.

REFERENCES

[1] N. Hoshimiya, *BioEngineering and Neuromuscular system*, Syoukoudou Press, Tyokyo, 1990.

[2] N. Hoshimiya, A. Naito, M. Yajima, and Y. Handa, "A multichannel FES system for the restoration of motor functions in high spinal cord injury patients: A respirations controlled system for multi-joint upper extremity," *IEEE Trans. on Biomedical Engineering*, vol. 36, pp. 754-760, 1989.

[3] A. R. Kralj and T. Bajd, *Functional Electrical*

Stimulation: Standing and Walking after Spinal Cord Injury, CRC Press Inc., Boca Raton, FL, 1989.

[4] G. Khang, and F. E. Zajac, "Paraplegic standing controlled by functional neuromuscular stimulation," *IEEE Trans. on Biomedical Engineering*, vol. 36, pp. 873-889, 1989.

[5] M. S. Hatwell, B. J. Oderkerk, C. A. Sacher, and G. F. Inbar, "The development of a model reference adaptive controller to control the knee joint of paraplegics," *IEEE Trans. on Automatic Control*, vol. 36, pp. 683-691, 1991.

[6] P. E. Cargo, H. J. Chizeck, M. R. Neuman, and F. T. Hambrecht, "Sensors for use with functional neuromuscular stimulation," *IEEE Trans. on Biomedical Engineering*, vol. 33, pp. 256-268, 1986.

[7] M. Levy, J. Mizrahi, and Z. Susak, "Recruitment, force and fatigue characteristics of quadriceps muscles of paraplegics isometrically activated by surface functional electrical stimulation," *Journal of Biomedical Engineering*, vol. 12, pp. 150-156, 1990.

[8] A. Stefanovska, L. Vodovnik, R. Stanislav, and R. Acimovic-Janezic, "FES and spasticity," *IEEE Trans. on Biomedical Engineering*, vol. 36, pp. 738-745, 1989.

[9] D. R. McNeal, R. J. Nakai, P. Meadows, and W. Tu, "Open-loop control of the freely-swinging paralyzed leg," *IEEE Trans. on Biomedical Engineering*, vol. 36, pp. 895-905, 1989.

[10] B. Flaherty, C. Robinson, and G. Agarwal, "Identification of nonlinear model of ankle joint dynamics during electrical stimulation of soleus," *Med. Biol. Comput.*, vol. 33, pp. 430-439, 1995.

[11] H. M. Franken, P. H. Veltink, and R. T. Henk, "Identification of passive knee joint and shank dynamics in paraplegics using quadriceps stimulation," *IEEE Trans. on Rehabilitation Engineering*, vol. 1, pp. 154-164, 1993.

[12] M. Ferrarin, F. Palazzo, R. Riener, and J. Quintern, "Model based control of FES-induced single joint movements," *IEEE Trans. on Neural Sys. Rehab. Eng.*, vol. 9, pp. 245-256, 2001.

[13] G. M. Eom, T. Watanabe, R. Futami, N. Hoshimiya, and Y. Handa, "Computer aided generation of stimulation data and model identification for FES control of lower extremities," *Front. Med. Biol. Eng.*, vol. 10, pp. 213-231, 2000.

[14] G. C. Chang, J. J. Luh, G. D. Liao, J. S. Lai, C. K. Cheng, B. L. Kuo, and T. S. Kuo, "A neuro-control system for the knee joint position control with quadriceps stimulation," *IEEE Trans. on Rehab. Eng.*, vol. 5, pp. 2-11, 1997.

[15] N. Lan, H. Q. Feng, and P. E. Crago, "Neural network generation of muscle stimulation patterns for control of arm movements," *IEEE Trans. on Rehab. Eng.*, vol. 2, pp. 213-224, 1994.

[16] G. M. Eom, *Generation of Optimal Stimulation for FES Standing Up using Computer Model Simulation*, Ph.D. dissertation, Department of Electronic Engineering, Tohoku University, Japan, 1999.

[17] G. Tao, and P. V. Kokotović, *Adaptive Control of Systems with Actuator and Sensor Nonlinearities*, John Wiley & Sons, Inc., 1996.

[18] A. Isidori, *Nonlinear Control Systems*, Springer-Verlag, London, 1995.

Gwang-Moon Eom received the B.S. degree in Electronic Engineering from Korea University, Seoul, Korea, in 1991. He received the M.S. degree and Ph.D. degree in Electronic Engineering from Tohoku University, Sendai, Japan in 1996 and 1999, respectively. Since 2000, he has been an Assistant Professor at the School of Biomedical Engineering, Konkuk University, Chungju, Korea. His research interests include assistive devices and technologies for the physically disabled and the elderly, the biomechanical system identification, and the application of artificial intelligence to biomechanical problems.

Jae-Kwan Lee received the B.S. and M.S. in Electrical Engineering from the Kyungpook National University, Daegu, Korea, in 1990 and 1993, respectively. He received the Ph.D. in Electrical and Communication Engineering from Tohoku University, Sendai, Japan, in 1998. Since then, he has been a Manager at Cartronics R&D Center, Hyundai Mobis, Kyounggi, Yongin, Korea. His research interests include robust adaptive schemes for uncertain nonlinear systems and their applications to advanced safety vehicles.

Kyeong-Seop Kim received the B.S. and M.S. degrees in Electrical Engineering from Yonsei University, Seoul, Korea, in 1979 and 1981, respectively. He received the M.S. degree in Electrical Engineering from Louisiana State University, Baton Rouge, in 1985 and the Ph.D. in Electrical and Computer Engineering from The University of Alabama in Huntsville, in 1994. He worked as a Principal Researcher of the Medical Electronics Laboratory at Samsung Advanced Institute of Technology, Kyounggi, Kiheung, Korea, from 1995 to 2001. Since March 2001, he has been a Faculty Member of the School of Biomedical Engineering, Konkuk University, Chungju, Korea. Dr. Kim was listed in Marquis Who's Who in Medicine and Healthcare, 2004-2005 & 2006-2007, Marquis Who's Who in Asia, 2006-2007, and the Cambridge Blue Book-2005. His research interests include physiological control modeling, biological signal analysis, medical image processing, and artificial neural networks.

Takashi Watanabe received the B.E. and M.E. degrees in Electrical Engineering from the Yamanashi University, Japan, in 1989 and 1991, respectively. He received the Ph.D. in Electronic Engineering from Tohoku University, Sendai, Japan in 2000. Since 2001, he has been an Associate Professor at the Information Synergy Center, Tohoku University, Japan. His research interests include neuromuscular control by FES, modeling of the musculoskeletal system and man-machine interface for paralyzed patients.

Ryoko Futami received the B.E., M.E., and Ph.D. degrees in Electronic Engineering from the Tohoku University, Japan, in 1980, 1982, and 1987, respectively. From 1982 to 1988, he had been a Research Associate at the Hokkaido University, Japan. He is currently a Professor in the Department of Human Support Systems at Fukushima University, Japan. His research interests include the analysis and modeling of temporal pattern processing and high-level brain functions, and also the control of paralyzed motor functions by FES.

A Basic Study of Fuzzy Controller for Cycle-to-Cycle Control of Knee Joint Movements of FES Swing: First Experimental test with a Normal Subject

T. Masuko [1], T.Watanabe [2], A.Arifin [3], M.Yoshizawa [2], N.Hoshimiya [4]

[1] Graduate School of Engineering, Tohoku University, Sendai, Japan
[2] Information Synergy Center, Tohoku University, Sendai, Japan
[3] Institute of Technology Sepuluh Nopember, Surabaya, Indonesia
[4] Tohoku Gakuin University, Sendai, Japan
masuko@yoshizawa.ecei.tohoku.ac.jp

Abstract

A feasibility of the fuzzy controller using cycle-to-cycle control for multi-joint movements of swing phase of FES-induced hemiplegic gait had been shown in our research group by computer simulation with musculoskeletal model. It was required to show the effectiveness of the fuzzy controller experimentally. In this study, a fuzzy controller using the cycle-to-cycle control method was tested experimentally in controlling the knee extension stimulating the Vastus using surface electrode stimulation. Experimental results with a healthy subject suggested that the fuzzy controller could realize the target maximum knee extension angle during walking.

1. INTRODUCTION

In the human motor functions, the movements of lower limbs during gait are complex multi-joint movements. So, an excellent FES control strategy is required to restore the paralyzed gait using FES. Our research group has studied an FES controller to develop the swing phase of hemiplegic gait in computer simulation towards improving gait ability.

We proposed the fuzzy controller based on the cycle-to-cycle control method for controlling swing phase of hemiplegic gait induced by FES [1]. Computer simulation study showed that the controller was feasible to control multi-joint (hip, knee, and ankle) movements of swing phase of FES-induced hemiplegic gait.

In this study, we focused on testing an effectiveness of the controller experimentally. As the basic study, experimental tests of the cycle-to-cycle control method were performed in controlling the knee extension angle with a normal subject.

2. METHODS

2.1 Control Algorithm

In the cycle-to-cycle control, stimulation burst duration TB is adjusted, while pulse amplitude, pulse width, and frequency of stimulation pulse are fixed. The adjustment of the burst duration TB is based on the performance of the previous cycle. Basic algorithm of the cycle-to-cycle control is shown in equation (1),

$$TB[n] = TB[n-1] + \Delta TB[n] \qquad (1)$$

where $TB[n]$ is the stimulation burst duration for the current cycle, $TB[n-1]$ is the stimulation burst duration of the cycle just before the current one, and $\Delta TB[n]$ is the output of the controller. Taking a controlling of the maximum knee extension angle for example, maximum knee joint angle obtained

in last control is used as a feedback signal. Error is defined as difference between target maximum joint angle and the obtained maximum joint angle.

2.2 Experimental Method

Knee joint angle of the left leg of a healthy subject (22 years old, male) was controlled by stimulating the Vastus (Vastus medialis, Vastus lateralis). The pulse width and the pulse frequency were 200μs and 20Hz, respectively. Electrical stimulation was applied to the muscles through the isolator and surface electrodes (F-150, Nihon Koden). The knee joint angle was measured with the goniometer (M180, Penny & Giles).

The subject sat on the chair that his leg didn't reach the ground and relaxed his legs during experiments. Before the controlling of the knee joint angle, maximum pulse amplitude was determined in order to get enough control range without pain, which was 50V in this case. The desired value of the maximum knee extension angle was set to 25 degree. A knee joint angle of 0 degree was defined as full extension. The knee joint angle at rest was about 90 degree. The cycle-to-cycle control was performed three times.

3. RESULTS

Figure 1 shows the result of the first trial of controlling the knee joint angle. The entire angle trajectory of the knee joint is given in Figure 1(a) with time on the x-axis and the knee joint angle on the y-axis. The obtained value of maximum joint angle at each cycle is plotted in Figure1 (b) with cycle number on the x-axis. Figure1(c) represents stimulation burst duration of each cycle.

In the first trial, although the result of the 19th cycle was not good, the maximum knee extension angle was controlled well most of the controlled cycles (Figure 1(b)).

Figure 2 shows result of the second trial of controlling the knee joint angle. In the second and the third trial, there were a few uncontrolled

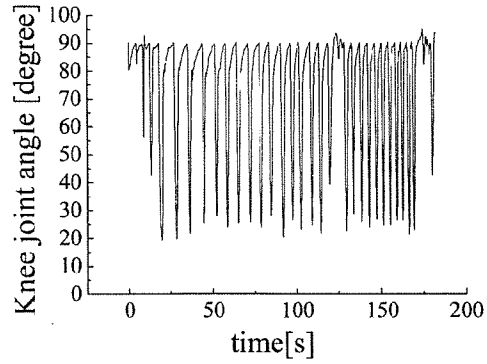

(a) entire trajectory of joint angle

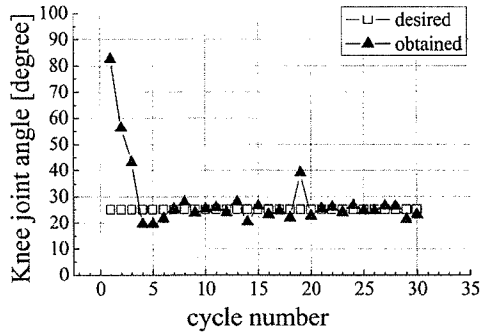

(b) obtained value of each cycle

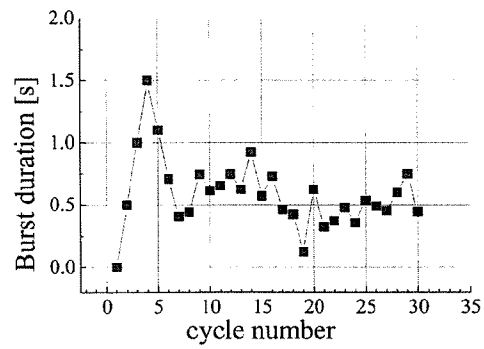

(c) burst duration

Figure 1 Results of the first trial of the cycle-to-cycle control of the knee joint angle. The maximum knee extension angle was controlled.

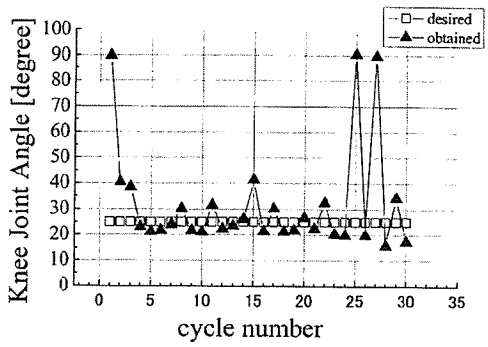

(a) obtained value of each cycle

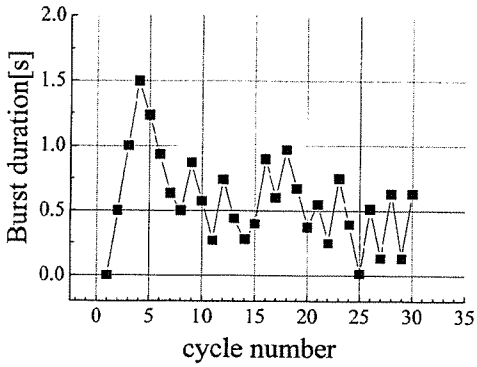

(b) burst duration

Figure 2 Results of the second trial of the cycle-to-cycle control of the knee joint angle.

cycles. They appeared in the cycle over 20th control as shown in Figure 2(a). However, the fuzzy controller recovered this uncontrolled situation by adjusting stimulation burst duration.

4. DISCUSSION AND CONCLUSION

Results of this paper suggested that the fuzzy controller using the cycle-to-cycle control would be effective in clinically. In this study, knee joint angle was controlled by stimulating single muscle (the Vastus). Our previous work using computer simulation showed that the controller could control multi-joint (hip, knee, and ankle) movements [1]. So, it is necessary to test the controller in controlling multi-joint movements experimentally.

In the experimental results, the knee joint didn't move sometimes (Figure 2(a)). The reason that the knee joint didn't move at the 25th cycle was considered that burst duration was very small. The maximum knee joint angle of the 24th cycle reached the target maximum joint angle, resulting in large reduction of the burst duration of the 25th cycle by the fuzzy controller. It is necessary to adjust the parameters of the fuzzy membership function for each subject.

On the other hand, muscle fatigue was considered to be a reason of the uncontrolled situation at the 27th cycle. Gradual decrease of muscle force caused by muscle fatigue was found to be compensated by the fuzzy controller in our previous simulation study [1]. However, sharp decrease of muscle force was not tested. It is necessary to study a method of dealing with such sudden change.

In this paper, the first experimental test was performed to study the effectiveness of the fuzzy controller. Methods of detecting the condition to start control and the maximum knee extension angle in each cycle were not considered strictly. The way of detecting maximum knee extension angle used in this paper was to compare each sampled data of joint angle after the end of electrical stimulation to the Vastus. There is a possibility that the detection method doesn't perform well because of disturbance, and so on. Development of practical methods will be necessary for clinical use.

Reference

[1] A.Arifin, T.Watanabe, N.Hoshimiya: Design of Fuzzy Controller of the Cycle-to-Cycle Control for Swing Phase of Hemiplegic Gait Induced by FES. IEICE Trans. Inf. and Syst, vol.E89-D, no.4: 1525-1533, 2006

Acknowledgements

This study was partly supported by the Ministry of Education, Culture, Sports, Science, and Technology, of Japan under a Grant-in-Aid for Scientific Research, and the Ministry of Health, Labour and Welfare under the Health and Labour Sciences Research Grants (Comprehensive Research on Disability Health and Welfare).

Development of Control Command Input Device Using Image Processing for FES system

Hiroki Higa[1], Satoshi Nishihara[1], Shin'ichiro Kanoh[2], and Nozomu Hoshimiya[3]

[1] University of the Ryukyus, Okinawa, Japan
[2] Tohoku University, Sendai, Japan
[3] Tohoku Gakuin University, Sendai, Japan

hrhiga@eee.u-ryukyu.ac.jp

Abstract

In this paper, a control command input device using image processing for functional electrical stimulation (FES) system is described. A CMOS camera was utilized in the device, and the eye movements were taken with it in real time. Control commands for FES system are a selection command, execution command and proportional control command. The eye movements such as the fixation, dextroversion, levoversion and supraversion, and the eye closure were selected. The input commands and eye movements were allocated as follows: the dextroversion and levoversion for the selection command, and the eye closure for the execution command. The dextroversion and levoversion were also allocated to the proportional control command in the execution mode. When getting back from the execution mode to the selection mode, the supraversion was used. Performance of the device was experimentally verified. The experimental results showed that this device was possible to use as an input device of FES system.

Key word: functional electrical stimulation (FES), image processing, eye movement, control command input device

1. INTRODUCTION

This paper deals with a control command input device using image processing for the functional electrical stimulation (FES) system. To restore the motor functions of the paralyzed extremities in spinal cord injury patients, FES is attracted the attention of people all over the world. The FES system consists of a stimulator unit, control command unit and some electrodes. The stimulator unit generates electrical stimulation according to the control command, electrical stimulation is conducted through the electrodes, and the users input their control commands to the stimulator using the control command unit. In this paper, the control command unit is focused.

Some control command units, for example, using shoulder movements [1], push switch [2], voice [3] and respiration [4], had been developed. However, there were some problems in these units. Therefore, we developed another control command input device in which CMOS camera were used to detect the eye movements for FES quadriplegic patients, and verified its operationality in the experiments.

2. METHODS

2.1. System Configuration

A configuration of the stimulator with the control command input device using image processing is shown in Fig. 1. This device is simply composed of a CMOS camera and image processing circuit. To detect the eye movements from images, image processing programs were made using Visual C++. The eye movements were taken with the CMOS camera.

In general, we have the eye movements shown in Fig. 2. To control the system shown in Fig. 1, the eye movements such as the fixation, dextroversion, levoversion and supraversion, and the eye closure were chosen. This is because these five movements can be intentionally generated. Control commands for FES system are basically composed of the following three commands: a selection command, execution command and proportional control command. The eye movements and input commands were allocated as follows: the dextroversion and levoversion for the selection command, and the eye closure for the execution command. The dextroversion and levoversion were also allocated to increase and decrease in quantity of the proportional control command in the execution mode, respectively. When getting back

from the execution mode to the selection mode, the eye movement in the supraversion direction was used.

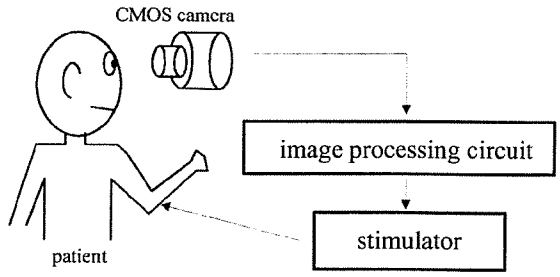

Figure 1 Configuration of stimulator with control command input device using image processing.

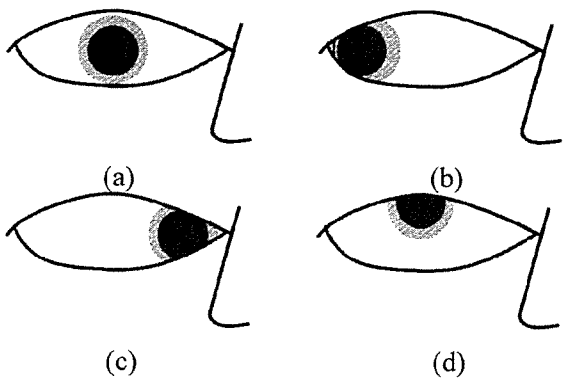

Figure 2 Detected eye movements: (a) the fixation, (b) dextroversion, (c) levoversion, and (d) supravertion, respectively.

2.2. Detection of the Eye Movements Using Image Processing

It is known that the color of the human skin has the characteristics of I-element in the YIQ color system. Thus, it is thought that it is possible to extract the eyes from images by paying attention to Y- and I- elements. In this paper, the RBG color system of an image was converted into the YIQ color system using the transform matrix

$$\begin{bmatrix} Y \\ I \\ Q \end{bmatrix} = \begin{bmatrix} 0.299 & 0.587 & 0.114 \\ 0.596 & -0.274 & -0.322 \\ 0.211 & -0.522 & 0.311 \end{bmatrix} \begin{bmatrix} R \\ G \\ B \end{bmatrix}. \quad (1)$$

The method applied to the image processing was the labeling. The steps of the image processing using labeling are as follows:

1. Read an image.
2. Transform an RGB image into YIQ format.
3. Binarize YIQ image.
4. Scan the binarized image and label connected pixel regions.
5. Find the longest connected pixed region in vertical direction and plot a point in its center.

After binarized, the binarized image was scanned from left to right, down to up, and connected pixel regions were labeled with the sequence number. At the end, the longest connected pixel region in the vertical direction was found, and a point was plotted in its center. A detection of the eye closures during blinks was set to the condition when the length of connected pixel regions was smaller than a certain threshold. In this case, the process that white pixels in the iris and pupil of the eye by the cause of the reflection of light were changed into black ones was added. For the labeling method, the Run Length method was utilized. This is both because a processing speed of a general labeling method was slow and becausc it was difficult to process images in real time. The Gray Level Run Length method [5] is a way to compress information. For a binary image, there are white pixels having the pixel values of 1 and black pixels having the pixel values of 0. Consecutive pixels of the same value in a given direction consist of a run. Thus, 2-dimensional region of binary image can be represented by the pixel value of 1 (or 0) and the sum of the run-lengths of 1s (or 0s).

2.3. Experiment

An experimental setup is shown in Fig. 3. A CMOS camera (USB-CAM 30V, I-O DATA DEVICE, Inc.) was fixed and movements of the right eye of an experimental subject, who was 24 years old, were taken with it. The distance between the right eye and the camera, and the resolution of images were set to 7.5 cm and 352 x 288 pixels, respectively. Using the image processing methods mentioned in the previous section, the obtained images were processed on the PC powered by the Pentium 4 processor of 2.8 GHz and RAM of 1 GB.

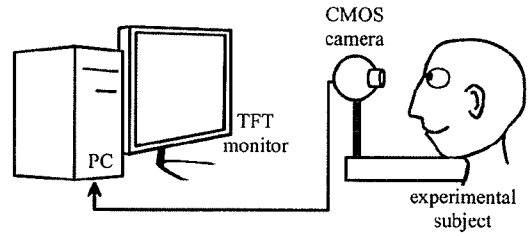

Figure 3 Experimental setup.

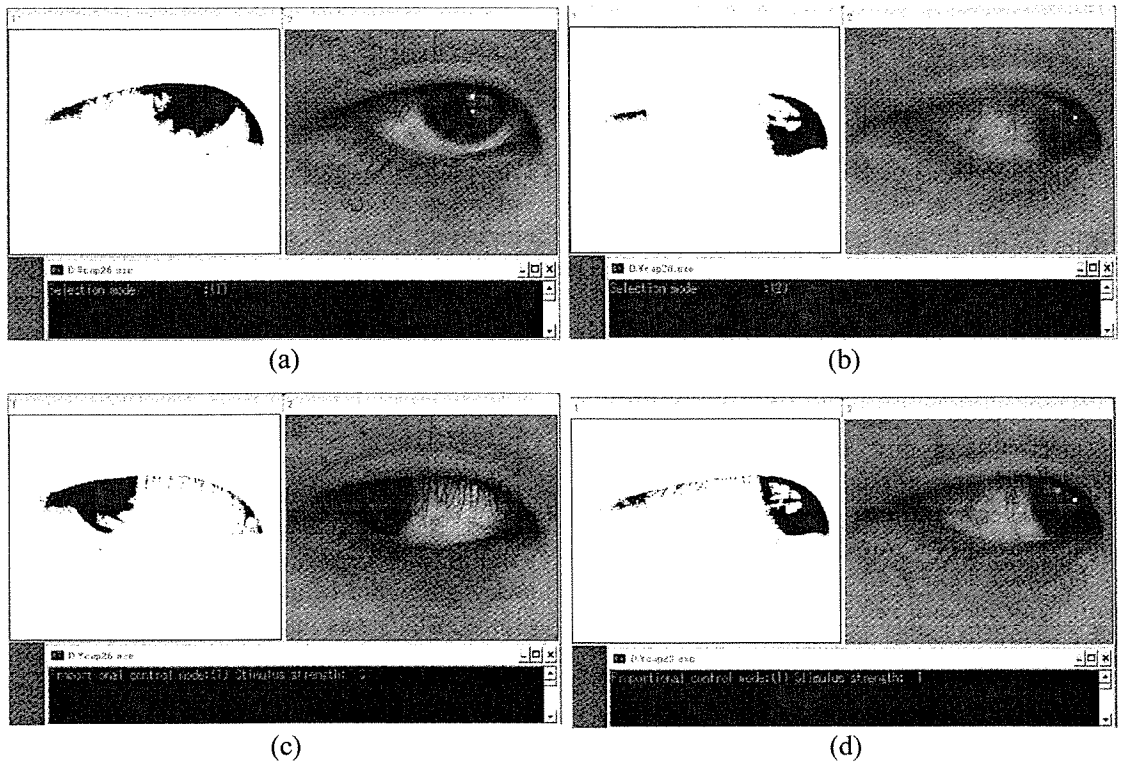

(a) (b)

(c) (d)

Figure 4 Experimental results of (a) initial condition (the fixation), (b) selection command (the levoversion), (c) increase in quantity of the proportional control command (the dextroversion), and (d) decrease in quantity of the proportional control command (the levoversion), respectively.

3. RESULTS

The experimental results are shown in Fig. 4. The left and right images are the results of doing image processing of the labelling and those of the resultant images. The control modes are indicated in the lower window. It was clear from the experimental results that not only the eye movements but the change in modes was distinctively detected. Furthermore, it was verified to get back from the execution mode to the selection mode by the supravertion.

4. DISCUSSION AND CONCLUSIONS

In this paper, the control command input device using the image processing for FES system was developed, and performance of the device was experimentally verified. The experimental results showed that it was possible to use as an input device of FES system. An experimental consideration of the stimulator with the control command input device should be needed for our future work.

References

[1] Y. Handa and N. Hoshimiya, "Restoration of motor function of paralyzed upper extremities by computer-controlled functional electrical stimulation (FES) system," *Trans. Jpn. Soc. Pathophysiology*, vol.6, no.4, pp.288-294, 1987.

[2] R. Kobetic, R.J. Triolo, J.P. Uhlir, C. Bieri, M. Wibowo, G. Polando, E.B. Marsolais, J.A. Davis, Jr., K.A. Ferguson, and M. Sharma, "Implanted functional electrical stimulation system for mobility in paraplegia: A follow-up case report," *IEEE Trans. Rehabil. Eng.*, vol.7, no.4, pp.390-398, 1999.

[3] Y. Handa, T. Handa, Y. Nakatsuchi, R. Yagi, and N. Hoshimiya, "A voice-controlled functional electrical stimulation system for the paralyzed hand," *Trans. Jpn. Soc. ME & BE,* vol.23, no.5, pp.292-298, 1985.

[4] A. Naito, Y. Handa, M. Yajima, H. Fukamachi, K. Ushikoshi, and N. Hoshimiya, "Development of new FES system controlled by inspiration and expiration for the paralyzed upper extremities," *Proc. Jpn. Soc. ME & BE, 1-D-8,* p.276, 1988.

[5] A. Chu, C. M. Sehgal, and J. F. Greenleaf, "Use of gray value distribution of run lengths for texture analysis," *Patt. Recogn. Lett.*, vol.11, pp.415-420, 1990.

Acknowledgements

This work was partially supported by the Ministry of Education, Science, Sports and Culture, Grant-in-Aid for Scientific Research (B).

Gait Re-education System for Incomplete Spinal Cord Injured Patients - Measurement of Hip Joint Angle by Piezoelectric Gyroscope -

Norio Furuse[1], Takashi Watanabe[2], Nozomu Hoshimiya[3]

[1]Miyagi National College of Technology, Japan
[2]Information Synergy Center, Tohoku Univcrsity, Japan
[3]Tohoku Gakuin University, Japan

E-mail: furuse@miyagi-ct.ac.jp

Abstract

In order to develop the FES rehabilitative system for re-education of walking, the sensor data that is necessary to give the information about the walking to the patients should be determined. In this paper, we examined measurement method of the hip joint angle simply by using gyroscopes. From the result of the walking analysis with the normal subjects, it was expected that the measurement system could measure the hip joint angle with sufficient accuracy.

1. INTRODUCTION

Functional electrical stimulation (FES) training of paralyzed muscles is effective for the great majority of incomplete spinal cord injured (SCI) patients in the early period of the rehabilitation process [1]. The aim of the FES system for re-education is not only to deliver the electrical stimulation to the paralyzed muscles, but also to evaluate the sensor information of the lower limb in order to give the useful information of the walking training to the patient [2], [3]. Therefore, in order to develop the FES rehabilitative system for re-education, the sensor data that is necessary to give the information about the walking to the patients should be determined. The joint angles of the lower limb in the walking training are important parameters to evaluate ability and stability of the walking [2]. We have shown the possibility of measuring knee and ankle joint angles by using plural gyroscopes that can be attached easily on the body [4], [5].

In this paper, we examined the simplified measurement method of the hip joint angle by using gyroscopes. The gyroscopes were attached to the trunk and the thigh for the measurement of the hip joint angle. Attachment position of the gyroscope to the trunk was also examined in walking experiment.

2. METHODS

To find out better attachment position of the sensor, four piezoelectric gyroscopes (Murata, ENC-03J) were attached to the trunk (chest: G1, umbilicus: G2, waist: G3 and lumbar: G4) and a gyroscope was attached to the right thigh (G5) as shown in Figure 1. Each gyroscope measured one-degree of angular velocity. The hip joint angle was calculated by using the outputs of the gyroscopes considering rigid-body dynamics as follows:

$$\theta_{hip} = \int(\dot{\theta}_{thigh} - \dot{\theta}_{trunk})dt \quad (1)$$

where $\dot{\theta}_{thigh}$ and $\dot{\theta}_{trunk}$ are angular velocity of the thigh and the trunk respectively. That is, the hip joint angle was calculated by the output of one of the four gyroscopes and that of G5. A trapezoidal rule was adopted as the method of numerical integration. A possible reason of error in the joint angle calculation was the offset in the outputs of the gyroscopes. In order to remove the error in the joint angle calculation, the influence by the offset

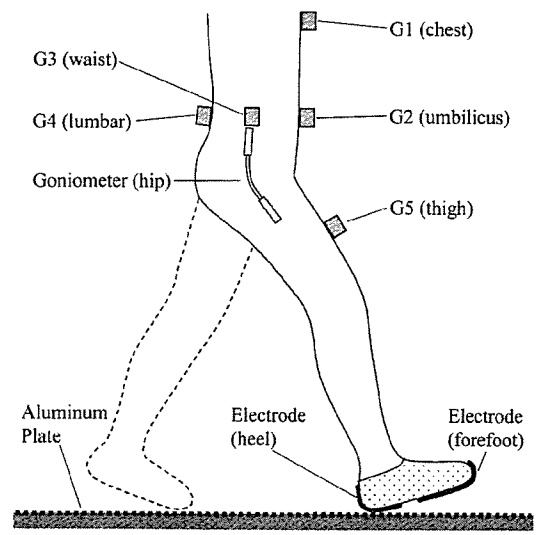

Figure 1: Attachment positions of the sensors for the measurement.

in the outputs of the gyroscopes was removed by the offline data processing. In order to evaluate the value of the joint angle calculated by the outputs of the gyroscopes, a goniometer (Penny & Gilles, ADU301A) was used to measure the hip joint angle simultaneously. The G1-G4 and the goniometer were attached on clothes and the G5 was attached directly on the skin. The sensor signals were amplified, low-pass filtered (2nd, 22.6Hz, Q=0.71) and sampled at 120 Hz.

Two aluminum electrodes and an aluminum plate were used to detect gait phases during the walking experiment. The foil form aluminum electrodes were attached to the forefoot and the heel of a shoe. The aluminum plate put on the floor was the length of 8 m with the width of 1 m. Four gait phases (mid stance, heel-off, swing and heel-strike) were detected by electric contact condition between the electrodes and the plate [4].

Three healthy subjects participated in the experiments. Their tasks were to walk with normal and slow speed on the aluminum plate. The subjects were able to do about 6-8 steps by the right leg in one trial of the walking. The measured data were analyzed offline using a personal computer.

3. RESULTS

The measured data together with the four gait phases were shown in Figure 2. The output of the gyroscope was different according to the attachment position of the trunk. The amplitude of the angular velocity measured by the gyroscope on the thigh (G5) was large compared to other ones.

The comparisons between the joint angle measured with the goniometer and calculated value by using the outputs of the gyroscopes were shown in Figure 3. The waveform of the joint angle calculated by the output of the gyroscopes looked like that measured with the goniometer. The difference of the joint angle between the calculation with the gyroscopes and the measurement with the goniometer was evaluated by Root Mean Square difference (RMS) and by correlation coefficient (CC). The RMS and the CC are shown in Table 1. The values of the RMS and the CC were mean values of 10 measured data under the condition of the normal speed walking. They showed that the gyroscopes could measure the hip joint angle as same as the goniometer. The G4 resulted in the smallest RMS and highest correlation in subject A and subject C, although there was no significant difference with t-test between result of the G4 and those of other gyroscopes. The same analysis for the data under the condition of the slow speed walking showed the similar results as those for the normal speed walking.

4. DISCUSSION

The value of the hip joint angle calculated by the gyroscopes was close to the measured value with the goniometer. The RMS and the CC in calculation of the hip joint angle using the G4

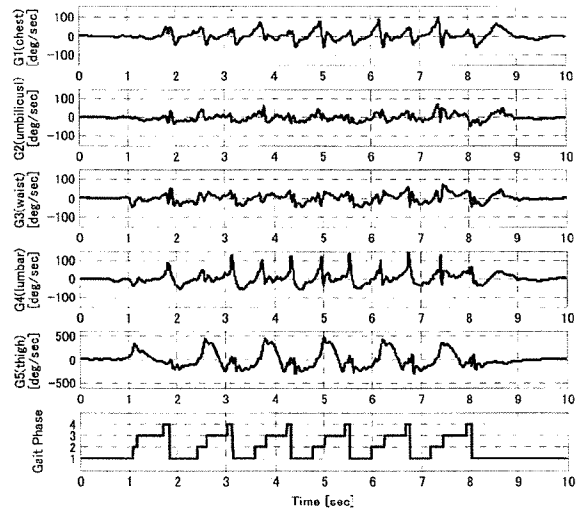

Figure 2: Angular velocities measured with the gyroscopes (subject A, normal speed walking). The attachment positions of each gyroscope were referred to the fig.1. Gait phase: 1) mid stance, 2) heel-off, 3) swing and 4) heel-strike.

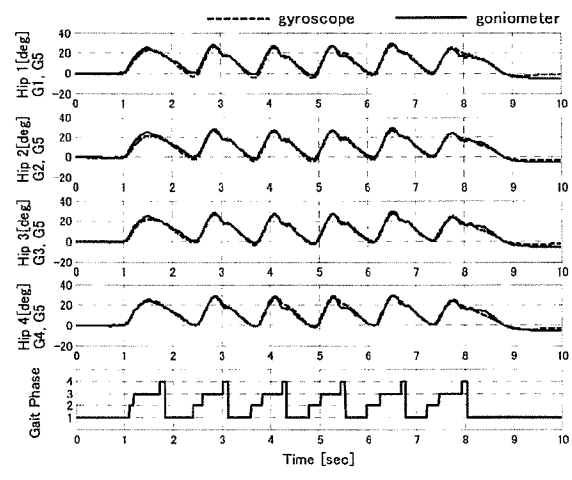

Figure 3: Comparison between the hip joint angle measured with goniometer and calculated value by using the outputs of the gyroscopes (subject A, normal speed walking). The gyroscopes used in the calculation: Hip1:G1&G5, Hip2:G2&G5, Hip3: G3&G5, Hip4:G4&G5. Gait phase: 1) mid stance, 2) heel-off, 3) swing and 4) heel-strike.

Table 1 The RMS and the CC between the hip joint angle calculated by the outputs of the gyroscopes and the one measured with the goniometer in normal speed walking.

gyro.	subject A		subject B		subject C	
	RMS	CC	RMS	CC	RMS	CC
G1,G5	1.87°	0.987	2.42°	0.970	2.73°	0.984
G2,G5	1.88°	0.987	2.79°	0.964	1.36°	0.988
G3,G5	1.61°	0.987	2.30°	0.973	1.40°	0.991
G4,G5	1.44°	0.991	2.44°	0.965	1.21°	0.991

were 1.70° and 0.982 respectively on the mean value of the three subject's data. These valucs were better than those of the knee (3.00°, 0.991) and the ankle joint angle (2.90°, 0.951) [5].

Two gyroscopes and one goniometer were attached together to one axis mechanical arm, and the angle was measurcd simultaneously when the arm opcrated [5]. As the result, there was a very small RMS and very high correlation (1.43°, 0.999) between the angle calculated by the outputs of the gyroscopes and the one measured with the goniometer. There was a little difference between the hip joint angle calculated by the outputs of the gyroscopes and the one measured with the goniometer in the walking experiment. The difference was considered to be caused due to the attachment of the sensors to the body.

5. CONCLUSIONS

In this paper, we examined the simple measurement method of the hip joint angle by using the gyroscopes attached to the trunk and the thigh. The result of the walking analysis with the normal subjects showed that the method could measure the hip joint angle with sufficient accuracy. It was also suggested that the lumbar region is preferable to attach the gyroscope on the trunk.

References

[1] T.Bajd, A.Kralj, M.Štefančič and N.Lavrač, "Use of Functional Electrical Stimulation in the Lower Extremities of Incomplete Spinal Cord Injured Patients," Artificial Organs, Vol.23, No.5, pp. 403-409, 1999.

[2] T.Bajd, I.Cikajlo, R.Šavrin, R.Erzin and F.Gider, "FES Rehabilitative Systems for Re-Education of Walking in Incomplete Spinal Cord Injured Persons," Neuromodulation, Vol.3, No.3, pp. 167-174, 2000.

[3] N.Furuse, I.Cikajlo and T.Bajd, "Training of foot contact phase during FES assisted walking," Proc. of the International Federation for Medical & Biological Engineering, pp.686-689, 2001.

[4] N.Furuse, T.Watanabe and N.Hoshimiya, "Gait Re-education System for Incomplete Spinal Cord Injured Patients -Measurement of Leg Joint Angles by Piezoelectric Gyroscope-," Proc. of the 9th Annual Conference of the International Functional Electrical Stimulation Society, pp.395-397, 2004.

[5] N.Furuse, T.Watanabe and N.Hoshimiya, "Simplified Measurement Method of Lower Limb Joint Angles by using Piezoelectric Gyroscopes," Trans. of the Japanese Society for Medical and Biological Engineering, Vol.43, No.4, pp.538-543, 2005(in Japanese).

Acknowledgments

This study was partly supported by the Ministry of Education, Culture, Sports, Science and Technology of Japan under a Grant-in-Aid for Scientific Research, and the Ministry of Health, Labour and Welfare under the Health and Labour Sciences Research Grants (Comprehensive Research on Disability Health and Welfare).

"BRAIN SWITCH" BCI SYSTEM BASED ON EEG DURING FOOT MOVEMENT IMAGERY

S. Kanoh[1], R. Scherer[2], T. Yoshinobu[1], N. Hoshimiya[3], G. Pfurtscheller[2]

[1]Graduate School of Engineering, Tohoku University, Sendai, Japan
[2]Institute for Knowledge Discovery, Graz University of Technology, Graz, Austria
[3]Tohoku Gakuin University, Sendai, Japan
E-mail: kanoh@ecei.tohoku.ac.jp

SUMMARY: EEG-based asynchronous brain-computer interface (BCI) system to realize binary switch by using simple thresholding of EEG beta band power was tested on six healthy subjects. EEG signal was measured from a bipolar channel on the vertex of the head, and was band-pass filtered, squared and smoothed on-line to extract the band power of beta oscillation. Subjects were requested to imagine foot movement, and if the band power exceeded a pre-defined threshold value, a command was generated. It was shown that two subjects out of six were able to induce bursts of beta oscillations by foot movement imagery, and binary commands could be detected in higher correct rates by these subjects.

INTRODUCTION

To provide better communication abilities to severely paralyzed patients, the EEG-based asynchronous (user-driven) brain-computer interface (BCI) that enabled binary switch by detecting the patients' foot motor imagery was studied.

We have developed a BCI to realize binary switch by detecting bursts of beta oscillation. Such a system, so called "Brain Switch", has been applied successfully to one paralyzed patient for controlling external FES (functional electrical stimulation) system [1].

In previous BCI studies, it was common to extract and classify features from preprocessed multi-channel EEG data by complex mathematical data analyses for increasing both information transfer rate and accuracy of the obtained commands. But for robust and easy-to-apply BCI for paralyzed patients, the binary switch with only a single channel would be reasonable.

In this study, the "Brain Switch" was tested on six healthy subjects to show the applicability of this system.

MATERIALS AND METHODS

Six healthy subjects took part in the experiments. From each subject, bipolar EEG (Cz-FCz) was measured by two Ag-AgCl electrodes with a forehead ground. Measured signal was amplified (sensitivity 50 μV) between 0.5 and 100 Hz with a biosignal amplifier and sampled with 250 Hz.

In the present method, the power increase of beta oscillation elicited by foot movement imagery was detected as a command. To estimate the band power of beta oscillation, signal was processed on-line by bandpass filtering (20–30 Hz), squaring and smoothing (moving average: 1 s). A white bar (power bar), whose length was propotional to the calculated power value, was displayed onto a LCD display as a feedback.

The experiments consisted of two parts. One was a free training session, in which subjects were requested to control the length of the power bar by foot movement imagery on his/her own pace. It was intended to help subjects to develop their own mental strategy for motor imagery. The other was a cue-based training session. Subjects were instructed to imagine foot movement during the presence of cue (from 0 to 6 s) onto the display, and to try and keep the length of the power bar longer during imagination.

To subjects with significant increase of beta band power during imagery, the free/cue-based training with command detection were applied. In these paradigms, the total numbers of desired/undesired detections were displayed together with the power bar. Beep signals were also presented when the events were detected as commands.

The criteria to detect events of motor imagery was as follows [1, 3]: An event was detected if the band power of beta oscillation exceeded a pre-defined threshold value for a certain time period (dwell time). To avoid undesired successive detections, refractory period was taken into account. These three parameters for command detection were initially set by ROC analysis [3], and were adjusted according to subjects' performances.

In this study, the change of beta band power due to foot movement imagery was evaluated for detecting commands. Generally, mu oscillation whose frequency range is similar to that of occipital alpha oscillation is also responsible to motor imagery. But this component was not used for detection, because it was very hard to separate it from alpha oscillation by using a single channel bipolar signal.

RESULTS AND DISCUSSION

From two subjects, significant bursts of ERS and ERD (event-related (de)synchronization [2]: increase and decrease of magnitude on specific frequency range) were observed. A weak ERD on wider frequency range (mu and lower beta bands) was observed from the rest four subjects.

An example of time-frequency map of EEG activity on cue-based training is shown in Figure 1. As shown in this figure, the following ERS and ERD components could be observed from those two subjects: (a) ERD after onset of motor imagery on lower beta band (20–25 Hz), which was related to motor planning, (b) sus-

tained ERS on upper beta band (25–30 Hz), (c) sustained ERD on mu band, (d) ERS after offset of motor imagery (rebound) on lower beta band.

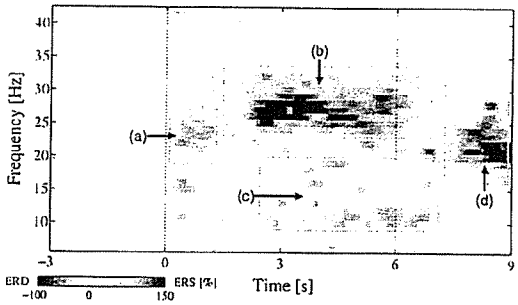

Figure 1: An example of time-frequency map of EEG activity related to foot movement imagery task during cue-based training for one subject. ERD (a and c), ERS (b and d).

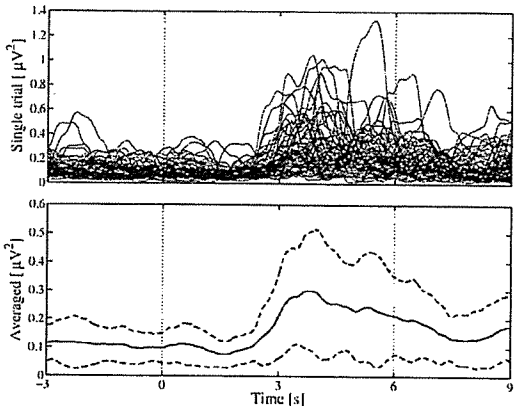

Figure 2: Single trial (upper) and averaged (lower, with standard deviation) band power of beta oscillation (25–30 Hz) induced by foot movement imagery for one subject.

Especially, the band power of upper beta range activities during foot motor imagery (b) was slightly stronger on these two subjects. The single-trial and averaged band power activities on this frequency range are shown in Figure 2 (results in Figure 1 and Figure 2 were given from the same data). As shown in this figure, an increase of upper beta (25–30 Hz) band power was observed from both single-trial and averaged activities.

The two subjects above participated in the experiments with command detection. Events were treated as true positives if it were detected during imagery period, otherwise they were treated as false positives. By these experiments, it was shown that the true events of foot motor imagery were detected with a probability of 60–90 %.

CONCLUSION

Applicability of the EEG-based asynchronous BCI system to realize a binary switch was tested on six subjects. It was shown that the bursts of EEG beta oscillations in the vertex of the head were induced by foot movement imagery on two subjects, and binary commands based on motor imagery could be detected in higher correct rates from these subjects. The present system detects foot motor imagery by simple thresholding, and it requires only one bipolar channel (three electrodes) for measurement. The "Brain Switch" would be a robust and easy–to–apply BCI system for paralyzed patients. Investigation of training effect and development of training strategies to improve the performance are left to future study.

REFERENCES

[1] Pfurtscheller G, Müller-Putz GR, Pfurtscheller J, Rupp R. EEG-based asynchronous BCI controls functional electrical stimulation in a tetraplegic patient. EURASIP Journal on Applied Signal Processing, 2005; 19: 3152–3155.

[2] Pfurtscheller G, Lopes da Silva FH. Event-related EEG/MEG synchronization and desynchronization: basic principles. Clin Neurophysiol, 1999; 110: 1842–1857.

[3] Townsend G, Graimann B, Pfurtscheller G. Continuous EEG classification during motor imagery - Simulation of an asynchronous BCI. IEEE Trans Neural Syst Rehab Eng, 2004; 12(2): 258–265.

片麻痺者の歩行遊脚期の cycle-to-cycle 制御に基づく FES 制御法：床反力を考慮したモデルシミュレーション

柴田　聡*　　渡邉　高志**,‡　　Achmad Arifin***　　吉澤　誠**　　星宮　望†

*　東北大学大学院工学研究科，仙台市青葉区荒巻字青葉 6-6-05
**　東北大学情報シナジーセンター，仙台市青葉区荒巻字青葉 6-6-05
***　Institute of Technology "Sepuluh Nopember", Surabaya 60111, Indonesia
†　東北学院大学，仙台市青葉区土樋 1-3-1
‡　email: nabe@isc.tohoku.ac.jp

要旨

我々は，これまで，機能的電気刺激（FES）を用いて片麻痺者の遊脚期を制御するための cycle-to-cycle 制御に基づくファジィ制御器を提案し，計算機シミュレーションによってその有効性を示してきた．しかし，簡単化のため，足部と床との接触を省略した遊脚のモデルを用いていたため，実際の応用を想定したモデル化が課題であった．そこで本報告では，立脚及び遊脚からなる筋・骨格モデルと床面モデルの構築を最初に行った．そして，ファジィ制御器による遊脚期の制御について，離床や着床を含めながら，構築したモデルを用いた計算機シミュレーションにより検討した．まず，ファジィ制御器の一部を改良し，筋・骨格系の特性が異なる患者にも適用可能にした．そして，床反力の影響がある場合でも，これまでに開発してきたファジィ制御器が有効であることを確認し，足関節底屈力に応じて刺激スケジュールを修正することがより有効になることを示した．

1．はじめに

我々の研究グループでは，機能的電気刺激（FES）による歩行再建において，cycle-to-cycle 制御に基づく片麻痺者の遊脚期の制御に着目してモデルシミュレーションによる検討を行ってきた[1]．これまでに，片麻痺者の麻痺側の遊脚期の股関節角度と膝関節角度と足関節角度を制御するファジィ制御器を提案し，その有効性を示してきたが，用いたモデルは麻痺側が遊脚期にある状態のみに着目し，立脚（健側）の運動は十分に遅いものとして遊脚（麻痺側）に推進力を与えないものと仮定し，簡略化したモデルであった．また，床面との接触を考慮していなかったため，離床や着床，麻痺側が遊脚期から立脚期に切り替わる状態の検討は行っていない．

本報告では，床面と足部の接触や麻痺側が遊脚期から立脚期へ切り替わる状態を含めて，計算機モデルシミュレーションにより FES 制御法について検討を継続するために，立脚（健側）が遊脚（麻痺側）に推進力を与えたり，床面との接触による床反力が与えられたりするモデルの構築を最初に行った．これを用いて，順動力学問題を解くことで麻痺側が遊脚期の状態における着床を含めた FES 歩行について，計算機シミュレーションにより検討を行った．

2．歩行モデルの構築

2．1　遊脚期の筋・骨格モデル

麻痺側が遊脚の場合の骨格モデルとして，図 1 のように，遊脚（麻痺側）の足，下腿，大腿，立脚（健側）の大腿，下腿の 5 つのセグメントと，それらを連結する左右の足関節と膝関節，股関節から構成した．なお，全ての関節は矢状面内のみに可動域を持つ蝶番関節とした．また，対象を歩行中の下肢に限定し，左右対称であること，立脚（健側）の足部は動作を通して地面に固定であることを仮定した．頭部や体幹，上肢は 1 つの質点で表現し，その全質量を股関節上に集中させ，上体の向きは鉛直方向とした．各セグメントの質量は，セグメントの中央に 1 つの質点として集中させた[2]．遊脚の足部については，足の甲の部分に質点を集中させたセグメントとしたが，図 2 に示すように，踵の位置は足関節からの長さ（L_f）を与えて決定した[3]．立脚の踵の位置も同様に決定した．関節トルクの符号は，全て反時計回りを正とした．セグメントの質量や長さなどのパラメータ値は文献[4]を用いた．

関節トルク τ は，電気刺激によるトルク τ_{CE} と受動粘弾性要素によるトルク τ_P の和として次式で求め

た[5].

$$\tau = \tau_{CE} + \tau_P \quad (1)$$

τ_{CE}は，電気刺激により発生する筋収縮力 F_{CE} とモーメントアーム（固定）との積により求め，F_{CE}は，筋の活動度，長さ－張力関係[6]，収縮速度－張力関係[7]，最大筋張力 F_{max} で表される Hill 型モデルにより求めた．なお，電気刺激による筋の活動度は，刺激強度に対する筋のリクルートメント特性[8]と活性化ダイナミクス[9]により求めた．受動粘弾性要素によるトルク τ_P は，文献[10]を参考にして各関節での運動毎に(2)式で記述し，これにより関節可動域も表現した．

$$\tau_p = -k_{i1}\exp\{k_{i2}(\theta_i + k_{i3})\} + k_{i4}\exp\{-k_{i5}(k_{i6} + \theta_i)\} - c_i\dot{\theta}_i \quad (2)$$

ここで，k_{i1} ～k_{i6} および c_i は，関節毎に異なる係数であり，文献[11]を参考にした．

運動方程式は Lagrange 法により導出した．モデルに使用した筋は，各関節での各運動における主動筋となるものを選択した（表 1）．

2．2　床面モデル

床面モデルは，つま先と踵の各々に働くとし，作用点に働く力の x 成分 f_g^x と y 成分 f_g^y を(3)式で表現した[11]．

$$f_g^x = \begin{cases} -k^G(x_g - x_g^0) - c^G\dot{x}_g & (y_g \le 0) \\ 0 & (y_g > 0) \end{cases}$$

$$f_g^y = \begin{cases} -k^G y_g + c^G f_{\max}(-\dot{y}_g) & (y_g \le 0) \\ 0 & (y_g > 0) \end{cases} \quad (3)$$

$$f_{\max}(x) = \max(x,0)$$

ここで，k^G，c^G は係数で踵とつま先で値が異なるとし，x_g, y_g は踵とつま先においてそれぞれ x_g^{heel}，y_g^{heel}，x_g^{toe}，y_g^{toe} として与えられる床反力作用点位置（図 2），x_g^0 は接地した瞬間の床反力作用点位置である．このモデルでは，立脚の踵の y 座標を 0 として与え，遊脚の足部の床反力作用点位置の y 座標が 0 以下ならば，床面モデルが作用するものとした．この床面モデルによって得られた床反力を(4)式により等価関節トルクに変換した[12]．

$$\boldsymbol{\tau} = \boldsymbol{J}^T\boldsymbol{F} \quad (4)$$

ここで $\boldsymbol{\tau}$ は各関節トルクのベクトル，$\boldsymbol{J}$ はヤコビ行列，$\boldsymbol{F}$ は作用点に働く力のベクトルである．

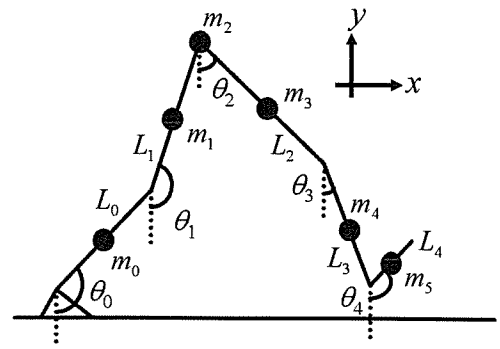

図 1　遊脚期の骨格モデル（θ_0～θ_4：鉛直方向からの振れ角，L_0 ～L_4：各セグメント長，m_0 ～m_4：各セグメント質量を集中させた質点）

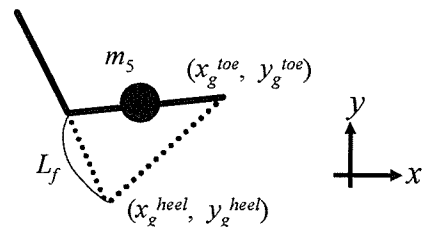

図 2　遊脚の足部における踵の位置および床面モデルの作用時の座標

表 1　モデルに含めた筋とその作用

主動筋	作用
ヒラメ筋	足関節の底屈
前脛骨筋	足関節の背屈
腓腹筋	足関節の底屈，膝関節の屈曲
大腿直筋	股関節の屈曲，膝関節の伸展
広筋群	膝関節の伸展
ハムストリングス	股関節の伸展，膝関節の屈曲
腸腰筋	股関節の屈曲
大臀筋	股関節の伸展

3．計算機シミュレーション

3．1　方法

前述の筋・骨格モデルを利用し，cycle-to-cycle 制御に基づくファジィ制御器[1]による遊脚期の制御に関する計算機シミュレーションを行った．片麻痺者を想定しているため，立脚（健側）の各関節角度は健常者の歩行時の立脚の股関節位置と膝関節位置の軌道を再現する角度をモデルに合わせて修正したものを入力し，遊脚の各関節角度の初期値は健常者の歩行における対応する関節角度と一致さ

せた.

cycle-to-cycle 制御では，電気刺激パルス列を印加する時間 TB を調整し，遊脚期の特徴的な点での角度を制御する．つまり，関節の最大屈曲角度などを制御対象とし，現在の cycle におけるその角度と対応する目標角度の誤差をフィードバック信号として次の cycle の TB を調整し，電気刺激を印加する．本研究で制御する関節角度は，歩行の遊脚期の股関節の最大屈曲角度，膝関節の最大屈曲角度，足関節の最大背屈角度と最大底屈角度，遊脚期の最終姿勢（着床）における各関節角度とした[1]．また，健常者の歩行時の関節角度を計測した結果から，各目標関節角度について歩行中の平均と標準偏差を算出し，その標準偏差を基に制御の許容誤差$\Delta\theta$を各制御対象について定め，関節角度誤差が$\pm\Delta\theta$の範囲に入ったら関節角度の制御ができているものと見なした[1].

ここで，本報告で構築した筋・骨格モデルでは，受動粘弾性要素のパラメータ値を文献[11]を参考に調整した結果，cycle-to-cycle 制御による足関節制御において最大底屈角度が検出されず，つま先が初期姿勢から最終姿勢に向けて重力の影響を受けて単調に底屈する場合があった．これに対して，健常者の歩行では，遊脚期の最大膝屈曲角度の約 70%の角度で足関節の最大底屈が生じていたことから，これを参考にして足関節制御器を改良した．つまり，n 歩（n cycle）目で足関節の最大底屈角度が検出されなかった場合，次の n+1 歩（n+1 cycle）目では，初期姿勢から膝関節の最大屈曲角度が検出されるまでの間で，膝関節角度（$\theta_{knee}[n+1]$）が一つ前の cycle での最大膝屈曲角度（$\theta_{knee\_max}[n]$）に対する 70%の角度に達すると，足関節の最大背屈角度に向けて前脛骨筋への電気刺激が印加されるように制御を変更した．なお，$\theta_{knee}[n+1]$が$\theta_{knee_max}[n]$の 70%に達する前に足関節の最大底屈が検出された場合には，それを優先させた.

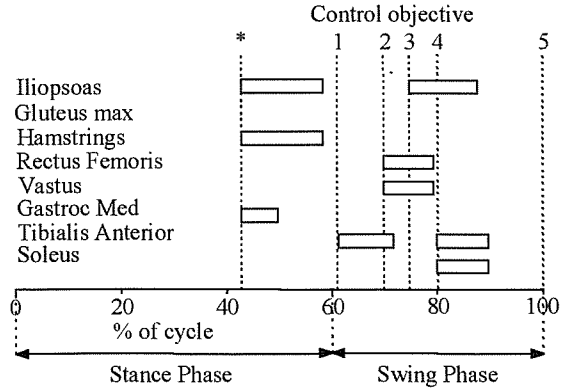

(a) これまでに作成されたスケジュール

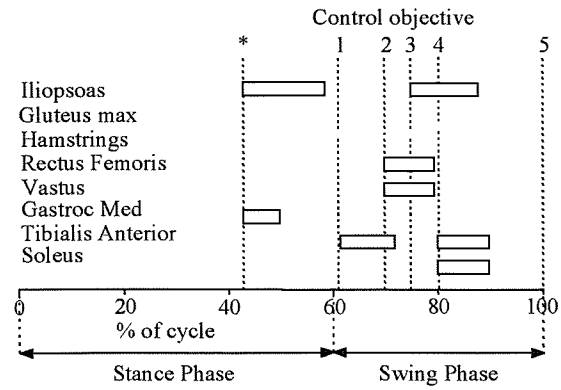

(b) ハムストリングスを除いた場合

図 3　電気刺激スケジュール
*：遊脚期開始，1：足関節の最大底屈角度の検出時，2：膝関節の最大屈曲角度の検出時，3：股関節の最大屈曲角度の検出時，4：足関節の最大背屈角度の検出時，5：遊脚期の最終姿勢（着床）

最初に，これまでの研究[1]と同様に，図 3(a)の電気刺激スケジュールを用いて，各筋の TB の初期値を 0 s として 50 歩分のシミュレーションを行った．被刺激筋は，先行研究[1]との比較のため，表 1 における大殿筋以外とし，電気刺激を印加した．ただし，ここでの計算機シミュレーションでは，床面モデルを適用しないで先行研究の制御法と改良型の制御法の比較を行った.

次に，改良型の制御法を用いて，床面モデルを適用して遊脚期制御の検討を行った．このとき，遊脚（麻痺側）に対して，筋が発生する関節トルクに加えて床反力による関節トルクが加わるため，遊脚期開始時にハムストリングスの電気刺激を印加する必要の無いことが考えられる．そこで，床反力を考慮した，より現実的な電気刺激スケジュールとして図 3(b)も検討した.

なお，計算機シミュレーションの時間ステップは 5×10^{-6} s とし，制御結果は 20 ms ごとに測定した．微分方程式の解法として 4 次のルンゲクッタ法を用いた．また，麻痺患者が数メートル歩いているうちに，制御された各関節角度が定常状態になっていることが望ましいと考え，ファジィ制御器の出力ファジィメンバシップ関数の値を，制御する各関節角度が 20 cycle 程度で定常状態に近づくように試行錯誤的に調整した.

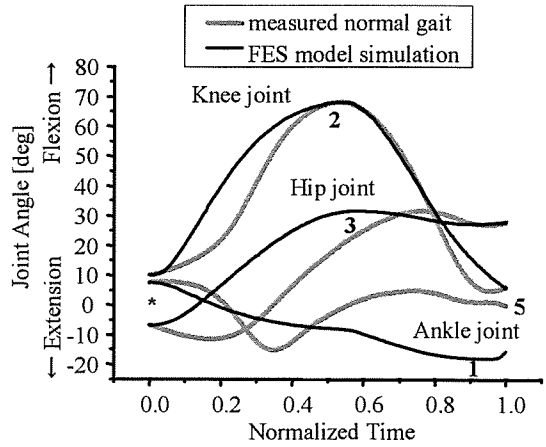

(a) 従来の制御器

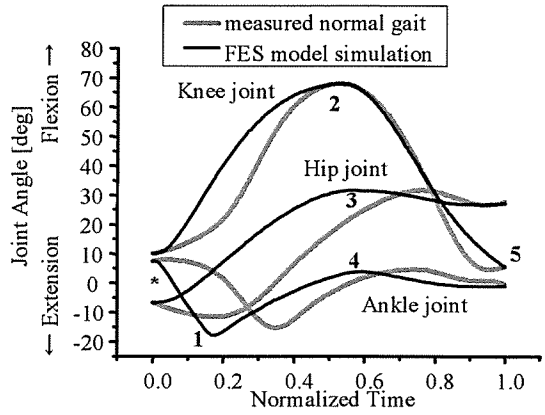

(b) 改良した制御器

図 4　床反力を考慮しない場合の制御結果．股関節角度：鉛直方向から屈曲方向を正，膝関節角度：大腿部の延長線と下腿部の為す角について屈曲方向を正，足関節角度：足部の甲と下腿部の延長線が為す角について 90° を 0° として屈曲方向を正としてプロットした．*，1～5 は，図 3 の control objective を参照．

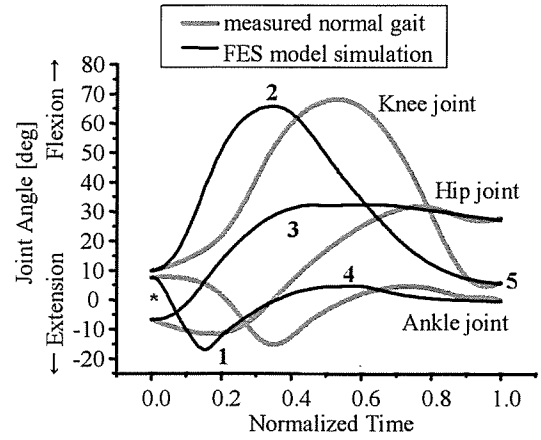

(a) 各関節の角度軌跡(角度の定義は図 4 を参照)

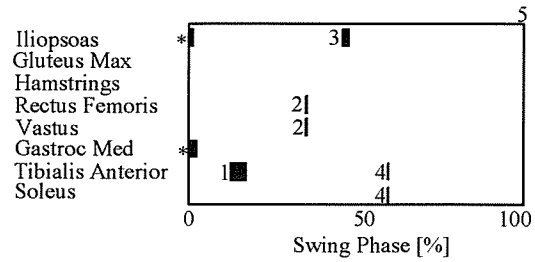

(b) 得られた電気刺激バーストパターン
*，1～5 は，control objective を表す．

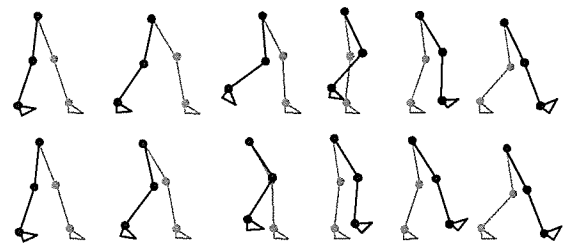

(c) 健常者（上）とモデル（下）の stick picture
（200ms 毎，黒：麻痺側，灰色：健側）

図 5　図 3(b)の電気刺激スケジュールによる 20 cycle 目の制御結果

3．2　結果

最初に，図 3(a)の刺激スケジュールを用いて，床面モデルを適用しない場合の従来の制御法と改良型の制御法による 20 cycle 目の制御結果の関節角度軌跡を図 4 に示す. 図 4(a)より, 従来の制御法では遊脚開始直後の最大底屈角度が検出されず, つま先が初期姿勢から最終姿勢に向けて重力の影響を受けて単調に底屈している様子を確認できる. 一方，足関節の制御器を改良した場合の制御結果が図 4(b)であり，足関節の最大底屈角度の制御が適切に行えることが確認できる．足関節の最大底屈角度の制御が適切に行われたことにより，その後の足関節の最大背屈角度および遊脚期の最終姿勢（着床）の角度の制御も適切に行えるようになり，患者の筋・骨格系の特性が変わっても改良型の制御法によって適切に制御を行えることを期待できる．

次に，床面モデルを適用した計算機シミュレーションにより改良型の制御法適用した結果では，いずれの刺激スケジュールでも 10 cycle 程度で制御角度が許容誤差範囲内に達することを確認でき，定常状態では，両方のスケジュールにより制御結果に差はみられなかった．ハムストリングスへの電気刺激を除去した電気刺激スケジュール（図 3(b)）を用いて制御した場合の 20 cycle 目の制御結果を図